MRI Signs of Parkinson's Disease and Atypical Parkinsonism

Magnetresonanztomografische Zeichen des idiopathischen Parkinson-Syndroms sowie atypischer Parkinson-Syndrome

Authors
Schekeb Aludin, Lars-Patrick Andreas Schmill

Affiliation
Clinic for Radiology and Neuroradiology, University Hospital Schleswig-Holstein – Campus Kiel, Germany

Key words
Parkinson's disease, atypical parkinsonism, MR imaging

received 30.10.2020
accepted 03.03.2021
published online 25.05.2021

Bibliography
Fortschr Röntgenstr 2021; 193: 1403–1409
DOI 10.1055/a-1460-8795
ISSN 1438-9029

Georg Thieme Verlag KG, Rüdigerstraße 14,
70469 Stuttgart, Germany

Correspondence
Schekeb Aludin
Clinic for Radiology and Neuroradiology, University Hospital Schleswig-Holstein – Campus Kiel, Arnold-Heller-Str. 3,
Haus D (Neurozentrum), 24105 Kiel, Germany
Tel.: +49/4 31/50 01 65 01
schekeb.aludin@uksh.de

ABSTRACT

Background Diagnosis of Parkinson's disease and atypical parkinsonism is based on clinical evaluation of the patient's symptoms and on magnetic resonance imaging (MRI) of the brain, which can be supplemented by nuclear medicine techniques. MRI plays a leading role in the differentiation between Parkinson's disease and atypical parkinsonism. While atypical parkinsonism is characterized by relatively specific MRI signs, imaging of Parkinson's disease previously lacked such signs. However, high-field MRI and new optimized MRI sequences now make it possible to define specific MRI signs of Parkinson's disease and have significant potential regarding differentiated imaging, early diagnosis, and imaging of disease progression.

Methods PubMed was selectively searched for literature regarding the definition and discussion of specific MRI signs of Parkinson's disease, as well as the most common types of atypical parkinsonism with a leading motor component. No time frame was set, but the search was particularly focused on current literature.

Results This review article discusses the different MRI signs of Parkinson's disease, multiple system atrophy, and progressive supranuclear palsy. The pathogenesis of the MRI signs is described, and imaging examples are given. The technical aspects of image acquisition are briefly defined, and the different signs are discussed and compared with regard to their diagnostic significance according to current literature.

Conclusion The MRI signs of Parkinson's disease, which can be defined with high-field MRI and new optimized MRI sequences, enable differentiated structural image interpretation and consecutive diagnostic workup. Despite the fact that the signs are in need of further validation by bigger studies, they have the potential to achieve significant diagnostic relevance regarding the imaging of Parkinson's disease and atypical parkinsonism.

Key Points:

- High-field MRI and specialized sequences make it possible to define specific MRI signs for neurodegenerative disorders
- Cerebral alterations can be detected in prodromal stages of Parkinson's disease
- The combination of specific MRI signs makes it possible to differentiate between Parkinson's disease and atypical parkinsonism

Citation Format

- Aludin S, Schmill LA. MRI Signs of Parkinson's Disease and Atypical Parkinsonism. Fortschr Röntgenstr 2021; 193: 1403–1409

ZUSAMMENFASSUNG

Hintergrund Die Diagnostik des idiopathischen Parkinson-Syndroms und der atypischen Parkinson-Syndrome basiert auf der klinischen Einschätzung der Patientensymptomatik und der gezielten Bildgebung mittels Magnetresonanztomografie, welche noch durch nuklearmedizinische Verfahren ergänzt werden kann. Die Bildgebung dient hierbei der Aufgabe der Differenzierung der verschiedenen Erkrankungen. Während atypische Parkinson-Syndrome recht spezifische MR-Zeichen aufweisen, ist das idiopathische Parkinson-Syndrom bildmorphologisch bisher eher als unspezifisch zu werten. Hohe Feldstärken und optimierte MR-Sequenzen ermöglichen jedoch neuerdings die Definition von spezifischen MR-Zeichen, welche Potenzial in der differenzierteren Bildgebung, der Frühdiagnostik und der Verlaufsdiagnostik des idiopathischen Parkinson-Syndroms hegen.

Methode Es erfolgte eine gezielte PubMed-Recherche mit Fokus auf Arbeiten zur Definition und Erörterung spezifischer MR-Zeichen des idiopathischen Parkinson-Syndroms sowie der häufigsten atypischen Parkinson-Syndrome mit führender motorischer Komponente. Es erfolgte keine Zeitraumbegrenzung bei besonderem Augenmerk auf aktuelle Literatur.

Ergebnisse Der vorliegende Übersichtsartikel erörtert die verschiedenen neuen MR-Zeichen des idiopathischen Parkinson-Syndroms sowie die bekannten Zeichen der Multisystematrophie und der progressiven supranukleären Blickparese. Die den Zeichen zugrunde liegende Pathologie wird jeweils definiert sowie bildmorphologische Beispiele gegeben. Es werden die technischen Aspekte der Untersuchungen kurz erörtert und die Zeichen anhand aktueller Literatur hinsichtlich der diagnostischen Wertigkeit zueinander verglichen.

Schlussfolgerung Die bei hohen Feldstärken und optimierten Sequenzen definierbaren MR-Zeichen des idiopathischen Parkinson-Syndroms ermöglichen eine differenziertere strukturelle Befundung und konsekutive Diagnostik. Die Zeichen müssen in größeren Studien weiter validiert werden, können jedoch künftig eine entscheidende diagnostische Relevanz in der Bildgebung der Erkrankungen aus dem Parkinson-Formenkreis bieten.

Introduction

Neurodegenerative diseases are a group of diseases affecting the central nervous system typically resulting in effects ranging from irreversible damage to the destruction of nerve cells. Epidemiologically speaking, the prevalence of these diseases increases significantly with age so that a substantial increase in the diagnosis of these diseases can be expected in the future in light of demographic changes. The diseases that are currently most common are the different forms of dementia and Parkinson's disease (PD) [1]. PD is characterized by the destruction of dopaminergic neurons in the substantia nigra (SN), which is part of the basal ganglia and is functionally associated with the extrapyramidal motor system. Patients affected by this disease have motor deficits characterized by the following key motor symptoms: akinesia, rigidity, tremor, and postural instability [2, 3]. The different types of atypical parkinsonism, e. g., multiple system atrophy (MSA) and progressive supranuclear palsy (PSP), as the most common types of atypical parkinsonism with a predominant motor component, have a similar clinical manifestation but differ pathogenetically and must be differentiated from PD. Diagnosis and differentiation of these diseases require dedicated clinical evaluation of the symptoms and represent a challenge for clinicians. Therefore, cerebral magnetic resonance imaging (MRI), which plays a significant diagnostic role in the differentiation between atypical parkinsonism and PD, is an important diagnostic tool [4]. To date, the PD has only been associated with nonspecific MRI signs in the clinical routine. However, recent studies have been able to define and determine new signs due to innovations in MRI techniques and sequences. In the future, in addition to currently established nuclear medicine methods like DaTSCAN and FDG-PET, these could have potential regarding the diagnosis of PD as well as differentiation from atypical parkinsonism [5–7]. Therefore, these MRI signs of PD are presented and explained in this overview. In addition, the MRI signs of the most important types of atypical parkinsonism are presented.

Parkinson's disease

In general, the cerebral MRI changes seen in Parkinson's disease are the result of the structural degeneration of dopaminergic neurons, which are primarily located in the SN of the mesencephalon. Histologically and functionally, this degeneration is characterized by destruction of the neurons with an increase in the total iron content in this area [8, 9]. These changes cannot be sufficiently visualized, and diagnostically significant MRI signs are difficult to define using conventional MR imaging with field strengths of less than three Tesla. However, field strengths of three Tesla and higher as well as modern sequences for imaging iron, specific neuropigments, and diffusion processes make it possible to visualize these changes, resulting in new MRI signs and parameters for evaluating the disease in terms of biomarkers [5–7]. These new MRI signs as a morphological imaging correlate of the neurodegeneration that occurs in PD are presented and explained in the following. However, it must be noted that these signs are not pathognomonic signs of PD but can also been seen in atypical parkinsonism.

Dorsal nigral hyperintensity

The increasingly precise visualization of anatomical structures via MRI makes it possible to better differentiate and evaluate neurofunctional structures, with the SN becoming increasingly relevant. The SN can be divided into the pars reticularis (SNpr) and the pars compacta (SNpc), with the SNpc housing the majority of the dopaminergic neurons in the central neuromotor system. The structural composition of the individual components is extremely complex. However, additional subregions in the SNpc known as nigrosomes can be defined. These are regions with a particularly high density of dopaminergic neurons and a proportionately low iron concentration. Of the five total nigrosomes (nigrosome-1 through 5), nigrosome-1 is the largest and is located in the dorsal section of the SNpc (▶ **Fig. 1a**) [10, 11].

High magnetic field strengths of three Tesla or higher and high-resolution iron-sensitive sequences like T2*-weighted sequences or susceptibility-weighted sequences (SWI) make it possible to also visualize these structures on MRI. Nigrosome-1 is visualized as a hyperintense, ovoid structure in the dorsolateral segment of the SNpc in these sequences. Since this region resembles a swallow tail on axial imaging of the mesencephalon, it is accordingly referred to as the "swallow tail sign" by some authors [12]. The neurodegeneration seen in PD results in the destruction of the dopaminergic neurons and an increase in the iron content

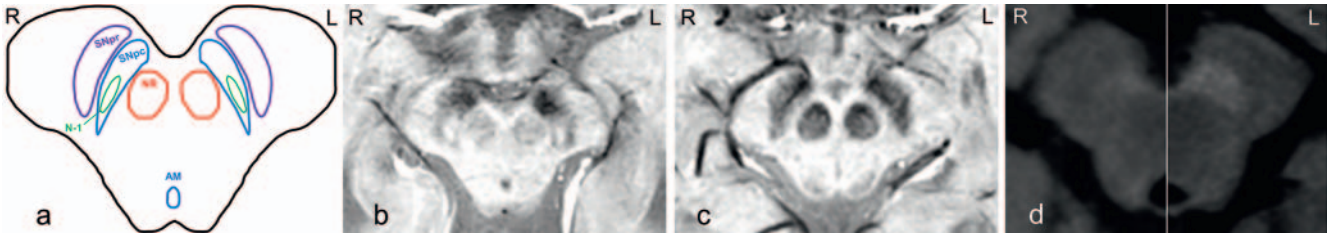

▶ **Fig. 1** Axial slice of the mesencephalon at the level of the substantia nigra. In the pictures, right (R) and left (L) are marked accordingly. **a** Illustration of mesencephalon, with the substantia nigra (SN), divided into the pars reticularis (SNpr) and pars compacta (SNpc), and the dorsal nigrosome-1 (N-1). Red nucleus (NR) and mesencephalic aqueduct (AM). **b** SWI sequence of a healthy control with physiological swallow tail sign by hyperintense nigrosome-1. **c** SWI sequence of a patient with Parkinson's disease with loss of swallow tail sign and reduced hyperintensity of nigrosome-1. **d** Two halves of an axial slice of the mesencephalon of a patient with Parkinson' disease (left) and of a healthy control (right) (T1-weighted, neuromelanin-sensitive sequence). Hyperintense signal of SNpc on the right as correlate of neuromelanin and reduced hyperintensity on the left as a sign of loss of neuromelanin.

in all nigrosomes. This occurs particularly clearly and early in nigrosome-1. It was able to be shown in this connection that nigrosome-1 or the physiological swallow tail sign is absent in iron-sensitive sequences (▶ **Fig. 1b, c**) [5, 11, 13]. The association between this absence of the swallow tail sign and PD has since been able to be confirmed in multiple studies and meta-analyses at high field strengths compared to healthy controls. Therefore, in 2017, Mahlknecht et al. were able to show a total sensitivity and specificity of 97.7 % and 96.4 %, respectively, in patients with PD compared to healthy controls in a meta-analysis of studies with field strengths of three and seven Tesla. In 2020, in another more recent meta-analysis, Chau et al. also found high values of 94 % and 90 % compared to healthy controls [14, 15]. However, it must be noted at this point that loss of the swallow tail sign is not to be interpreted as pathognomonic for PD. This sign was also able to be detected in additional studies regarding different types of atypical parkinsonism like multiple system atrophy (MSA) and progressive supranuclear palsy (PSP). Therefore, differentiation of the diseases on the basis of this sign alone is not recommended and additional morphological imaging criteria of atypical parkinsonism should be used [16–18]. In addition to the higher sensitivity and specificity compared to healthy controls, it is interesting that a bilateral decrease in hyperintensity can typically be additionally seen in PD patients at higher field strengths while this decrease tends to be unilateral on the dominant symptom side at three Tesla. The differences can probably be attributed to the better spatial resolution at higher field strengths so that findings can be evaluated in greater detail. In addition to the detection of this phenomenon in patients with PD, the relatively early change in nigrosome-1 is also a potential and interesting biomarker for early or prodromal phases of the disease. In a study in 2017, Yung Bae et al. were able to show a corresponding phenomenon in a small cohort of patients with idiopathic REM sleep behavior disorder (iRBD). According to current knowledge, this disorder represents a possible prodromal phase of PD and the authors show a significantly greater incidence of this phenomenon in patients with iRBD relative to the healthy control group (HC) [19]. However, the results of the available studies must be viewed in consideration of multiple aspects For example, the acquisition technique of the SWI sequences must be taken into account. A standardized sequence protocol has not yet been established in the literature. In a current overview by Kim et al. evaluating technical questions regarding nigrosome-1 imaging via SWI techniques, the authors state that slice thicknesses between 0.7 and 2.4 mm have been used in relevant studies. Based on their experience, the authors recommend a spatial resolution of $0.5 \times 0.5 \times 1\ mm^3$ for good resolution and contrast-to-noise ratio. However, they also state that optimized clinical studies are needed to establish a standardized protocol for SWI imaging of nigrosome-1 [22].

Neuromelanin

Neuromelanin (NM) is a pigment protein that is characteristically seen in specific brain regions in humans like the SN and the locus coeruleus (LC). It is produced during the oxidation of dopamine and has the ability to bind iron and other metals on an intracellular level. However, extracellular neuromelanin caused by cell death can result in neuroinflammatory processes [20, 21]. The amount of NM follows a typical age-dependent trajectory [23].

With the introduction of NM-sensitive MRI sequences by Sasaki et al. [6], NM has become increasingly important and has been increasingly used in studies regarding the diagnosis of Parkinson's disease and the differentiation of PD from essential tremor (ET) and atypical parkinsonism. The paramagnetic properties of NM which cause shortening of the T1 time in T1 turbo-spin-echo sequences are used here (▶ **Fig. 1d**) [24, 25]. Numerous studies describe a high specificity and sensitivity of a decreased amount of NM in the SN and the LC with respect to differentiating between patients with PD and healthy controls (HC). Moreover, combining the amount of NM and quantitative susceptibility mapping (QSM) allowed differentiation of patients with ET from untreatable patients with PD [24]. Studies examining the amount of NM over the course of PD showed that NM is already decreased in the early stages of the disease but then remains at a constant low at a certain point over the course of the disease. This allows differentiation between patients in early and late stages of the disease. However, the amount of NM does not correlate with disease progression [26]. There are promising results indicating that neuromelanin can be used as a marker for early detection particularly in the early stage and in the preliminary stages of PD. iRBD seems to correlate with a decreased amount of NM in the LC. Therefore,

the amount of NM in PD patients compared to healthy controls is significantly decreased but is also significantly lower in iRBD-positive PD patients compared to iRBD-negative patients [27]. Based on NM imaging combined with other sequences, it is also possible to differentiate iRBD patients from healthy controls [28]. Damage in the LC is also hypothesized as one of the causes of REM sleep behavior disorder [29].

Initial studies also show possible differentiation between PD, HC, and types of atypical parkinsonism like MSA and PSP using deep learning algorithms. However, this still needs to be confirmed on the basis of larger cohorts [30].

Iron content

Like NM, iron, which is usually bound to NM or ferritin, is also found in specific regions of the brain [9]. In a healthy person, the highest iron concentrations are found in the putamen (PUT), the globus pallidus (GP), and the nucleus caudatus (NC) and smaller amounts are found in the SN and LC. Examinations of healthy subjects show that the iron content in the LC remains largely constant over a lifetime, while it increases linearly with age in the SN.

However, atypical iron concentrations usually in terms of an accumulation are seen in numerous neurodegenerative diseases like PD or Alzheimer's disease (AD). To date, it is still unclear whether the iron deposits are the primary or a secondary event. However, it has been shown that iron deposits also result in accumulation of alpha-synuclein and the formation of fibrils near the nucleus [31]. Magnetic resonance imaging takes advantage of the T2-shortening effect of iron resulting in clear demarcation in T2- and T2*-weighted sequences. However, more precise mapping is possible with R2 (R2 = 1/T2) and R2* (R2* = 1/T2*) [29]. Sensitive visualization of iron is also possible using SWI or new methods like QSM which have already provided realistic quantification of iron content in postmortem studies [32].

Many studies comparing these parameters between PD patients and HC describe significant differences with an increased iron content in PD patients in the SN in SWI [33] as well as R2 / R2* and QSM. It has been shown multiple times that QSM is more sensitive than R2* [7, 34]. However, some contradictory results have been published with respect to QSM in other regions of the brain. This may be able to be attributed to various disease stages in the patients who were examined. Among others, the SNpc, the GP internus, the PUT, the NC, and the red nucleus (NR) have been described as regions with increased concentrations [35]. With a focus on the SN and the time curve of iron concentrations, a significant increase in R2* values in the SNpc within a period of 18 months with a good correlation with the progression of non-motor symptoms is seen in patients with advanced PD with a disease duration of more than five years [36]. Ulla et al. also examined the curve of R2* values for a period of 3 years and detected a significant increase in values in the SNpc and SNpr in PD patients, with the delta R2* values correlating positively with the increase in the UPDRS III score [37]. Langkammer et al. also describes a correlation of the QSM with the UPDRS but also with the Hoehn & Yahr Score and the Levodopa-equivalent daily dose (LEDD) [7]. Thus, the detection of iron in the basal ganglia via R2* and QSM is a promising technique for diagnosing PD and for evaluating progression. However, multicenter and longitudinal studies are needed to validate the results. Initial approaches using these self-learning analysis methods to differentiate atypical parkinsonism from PD have yielded promising results [38].

Diffusion-weighted imaging

Diffusion-weighted imaging is already part of the clinical imaging routine in neurodegenerative diseases. Diffusion tensor imaging (DTI) detects characteristics like fractional anisotropy (FA) and mean diffusion (MD). Meta-analyses have shown that significant differences between patients with PD and HC can be found with these techniques [39, 40]. The main features here are decreased FA and/or increased MD in the SN, the corpus callosum, the frontal lobes, the cingulum, and the temporal cortex. Additions to this technique, like Bi-tensor DTI, which takes the effect of free water into consideration, provide increasingly precise results [41] [24] and detect significant increases in free water in the posterior SN, which are also an indication of cell death in PD [42].

Newer methods like diffusion kurtosis imaging (DKI), which also detects the non-Gaussian distribution of water, or NODDI (neurite orientation dispersion and density imaging), which allows specific characterization of tissue microstructure, provide new insight into the changes seen in neurodegenerative diseases. There have been few studies to date addressing DKI in the SN [43, 44], but the available studies describe a significant increase in the kurtosis in the SN, which correlates positively with the Hoehn & Yahr score and the UPDRS III [43].

Multiple system atrophy

MSA is an α-synucleinopathy and is characterized by typical oligodendroglial cytoplasmic inclusion bodies. In addition to pronounced autonomic dysfunction, the symptoms of MSA are similar to those of PD in many cases, which often makes clinical differentiation from other parkinsonian syndromes difficult. Depending on the symptoms, a differentiation is made between MSA-P (Parkinsonian type) and MSA-C (cerebellar type) [45]. There are several ways to further define the appearance of the syndromes on MRI.

The characteristic features of MSA-P are atrophy of the putamen with a bilateral "putaminal rim sign", which represents a T2 hyperintense border of the dorsolateral putamen (▶ **Fig. 2a**), as well as a fundamental T2 hypointensity and atrophy of the putamen. Atrophy of the middle cerebellar peduncle (MCP), the cerebellum, and the pons, the hot-cross bun sign indicating T2 hyperintensity of the pons (▶ **Fig. 2b**), and the MCP sign indicating T2 hyperintensity of the MCP are the main characteristic features of MSA-C [46]. These characteristic atrophy patterns can be detected based on an increased midbrain-to-pons ratio (MTPR; area ratio of M to P in the median sagittal slice, shown as an example in ▶ **Fig. 2c**) or based on a low magnetic resonance parkinsonism index (MRPI; (area of P × diameter of MCP)/(area of M × diameter of the SCP)) [45, 47]. Based on the MRPI, MSA-P can be differentiated from PD or PSP [47]. Moreover, the various disease groups can be differentiated on the basis of diffusion-weighted imaging which shows significantly elevated ADC values in the MCP in MSA-P [45]. A combination of the T2* relaxation rates in the putamen can be used to differentiate between MSA-P and PD [48].

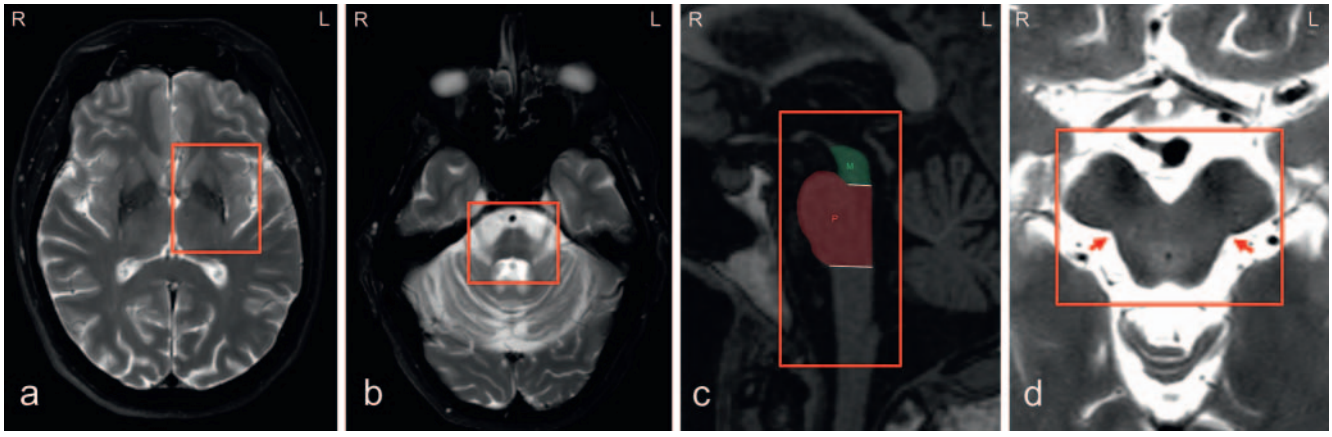

▶ **Fig. 2** Several MRI signs for multiple system atrophy (MSA) and progressive supranuclear palsy (PSP). **a** Axial T2-weighted image showing putamen with hyperintense border of the dorsolateral part on the left as putaminal rim sign. **b** Axial T2-weighted image showing pons with hyperintense hot-cross bun sign. **c** Sagittal T1-weighted image of the brainstem showing atrophy of the mesencephalon and the hummingbird sign. The areas for determining the MTPR are drawn here as an example. M: Midbrain; P: Pons. **d** Axial T2-weighted image of the mesencephalon with pronounced lateral atrophy of the tegmentum and Mickey Mouse sign.

Progressive supranuclear palsy

Progressive supranuclear palsy (PSP) is a tauopathy and is characterized by the deposition of tau proteins in brain tissue as well as neurodegeneration and atrophy in the basal ganglia, the brain stem, and the cerebellar nuclei. Based on the clinical appearance, multiple sub-types can be differentiated, with the most common being Steele-Richards Syndrome (PSP-RS) and Parkinson-predominant PSP (PSP-P). PSP-RS is associated with hypokinetic-rigid motor function, early postural instability, vertical gaze palsy, and impaired cognition. PSP-P is characterized by predominantly hypokinetic-rigid motor function and a late onset of additional symptoms like gaze palsy [49].

Differentiation from PD is based on clinical findings and MR imaging. However, the new signs of PD described above according to currently available studies can only be applied with caution since both the amount of neuromelanin and the hyperintensity of the dorsolateral portion of the SNpc can also be decreased in iron-sensitive sequences in PSP. Reliable differentiation on the basis of these signs alone is therefore difficult and the significance of the currently available studies is not yet fully clear [18, 50].

Based on the atrophy pattern occurring primarily in the midbrain in PSP, special signs that can be visualized on conventional MR imaging can be defined. Sagittal sequences through the brain stem and mesencephalon make it possible to detect the hummingbird sign in which the morphology of the structures resembles the silhouette of a hummingbird as a result of atrophy of the tegmentum (▶ **Fig. 2c**). An axial slice of the tegmentum of the midbrain in corresponding sequences reveals laterally pronounced volume loss in this region, resulting in a silhouette resembling Mickey Mouse in the midbrain. The sign is therefore called the Mickey Mouse sign by some authors (▶ **Fig. 2d**). In the literature these signs have high specificity but only moderate sensitivity. For example, in 2018 in a large retrospective analysis including 481 patients with neurodegenerative diseases (85 patients with PSP and 79 healthy controls), Mueller et al. found a high specificity of 99.5 % for the hummingbird sign and 97.7 % for the Mickey Mouse sign but proportionately low sensitivities of 51.6 % and 38.6 %, respectively [51]. In addition, evaluation of whether these signs can be detected at an early stage of the disease and should be used for early diagnosis is of particular interest. A corresponding work group examined a subgroup of patients that could not be definitively clinically diagnosed at the time of imaging. With respect to subsequent clinical diagnosis of PSP within this subgroup, they found a specificity of 100 % for both signs but only a low sensitivity of 35.3 % [52]. In addition to qualitative detection of midbrain atrophy based on corresponding MRI signs, an additional quantitative approach to detecting atrophy pattern has proven useful. Therefore, determination of the above-mentioned MRPI based on the pronounced atrophy primarily in the superior cerebellar peduncle in PSP (especially PSP-RS) allowed good differentiation from MSA-P and PD with excellent specificity and sensitivity [52, 53]. The quantitative approach using MRPI also seems to have certain potential regarding early diagnosis. Therefore, in a study in 2016, Quattrone et al. were able to show that a pathological MRPI in PSP-P patients has a better correlation with the development of vertical gaze palsy than symptoms like postural instability or vertical ocular slowness [54]. However, there are not many studies currently on this topic and additional studies are needed to evaluate this potential more closely.

Summary

MR imaging is an important tool for diagnosing and differentiating neurodegenerative diseases among Parkinson's-like diseases. In addition to the atrophy patterns that are already established for differentiating between the different types of atypical parkinsonism, new MRI signs have potential regarding differentiated diagnosis and follow-up. Therefore, the loss of DNH, decreased neuromelanin in the SNpc and in the LC, an increase in iron deposits, and impaired diffusion in the SNpc can be used for the diagnosis

of PD. The loss of DNH and a decrease in neuromelanin could contribute to early detection already in the prodromal phase. Iron quantification and diffusion kurtosis imaging can be used for the monitoring PD. However, these signs must be further validated in longitudinal and multicenter studies. An interesting future aspect is the development and application of artificial intelligence in this field which will increase the reliability of early diagnosis based on multifactorial image interpretation.

Conflict of Interest

The authors declare that they have no conflict of interest.

References

[1] de Lau LML, Breteler MMB. Epidemiology of Parkinson's disease. The Lancet Neurology 2006; 5: 525–535. doi:10.1016/S1474-4422(06)70471-9

[2] Reith W. Neurodegenerative Erkrankungen. Radiologe 2018; 58: 241–258. doi:10.1007/s00117-018-0363-y

[3] Kovacs GG. Molecular Pathological Classification of Neurodegenerative Diseases. Turning towards Precision Medicine. Int J Mol Sci 2016; 17: doi:10.3390/ijms17020189

[4] Erkkinen MG, Kim MO, Geschwind MD. Clinical Neurology and Epidemiology of the Major Neurodegenerative Diseases. Cold Spring Harb Perspect Biol 2018; 10: a033118 doi:10.1101/cshperspect.a033118

[5] Blazejewska AI, Schwarz ST, Pitiot A et al. Visualization of nigrosome 1 and its loss in PD. Pathoanatomical correlation and in vivo 7 T MRI. Neurology 2013; 81: 534–540. doi:10.1212/WNL.0b013e31829e6fd2

[6] Sasaki M, Shibata E, Tohyama K et al. Neuromelanin magnetic resonance imaging of locus ceruleus and substantia nigra in Parkinson's disease. Neuroreport 2006; 17: 1215–1218. doi:10.1097/01.wnr.0000227984.84927.a7

[7] Langkammer C, Pirpamer L, Seiler S et al. Quantitative Susceptibility Mapping in Parkinson's Disease. PLoS ONE 2016; 11: e0162460 doi:10.1371/journal.pone.0162460

[8] Dickson DW. Neuropathology of Parkinson disease. Parkinsonism Relat Disord 2018; 46 (Suppl. 1): S30–S33. doi:10.1016/j.parkreldis.2017.07.033

[9] Ward RJ, Zucca FA, Duyn JH et al. The role of iron in brain ageing and neurodegenerative disorders. The Lancet Neurology 2014; 13: 1045–1060. doi:10.1016/S1474-4422(14)70117-6

[10] Damier P, Hirsch EC, Agid Y et al. The substantia nigra of the human brain. I. Nigrosomes and the nigral matrix, a compartmental organization based on calbindin D(28K) immunohistochemistry. Brain 1999; 122: 1421–1436. doi:10.1093/brain/122.8.1421

[11] Lehéricy S, Bardinet E, Poupon C et al. 7 Tesla magnetic resonance imaging. A closer look at substantia nigra anatomy in Parkinson's disease. Mov Disord 2014; 29: 1574–1581. doi:10.1002/mds.26043

[12] Schwarz ST, Afzal M, Morgan PS et al. The 'Swallow Tail' Appearance of the Healthy Nigrosome – A New Accurate Test of Parkinson's Disease. A Case-Control and Retrospective Cross-Sectional MRI Study at 3T. PLoS ONE 2014; 9: e93814 doi:10.1371/journal.pone.0093814

[13] Schwarz ST, Mougin O, Xing Y et al. Parkinson's disease related signal change in the nigrosomes 1–5 and the substantia nigra using T2* weighted 7T MRI. Neuroimage Clin 2018; 19: 683–689. doi:10.1016/j.nicl.2018.05.027

[14] Mahlknecht P, Krismer F, Poewe W et al. Meta-analysis of dorsolateral nigral hyperintensity on magnetic resonance imaging as a marker for Parkinson's disease. Mov Disord 2017; 32: 619–623. doi:10.1002/mds.26932

[15] Chau MT, Todd G, Wilcox R et al. Diagnostic accuracy of the appearance of Nigrosome-1 on magnetic resonance imaging in Parkinson's disease. A systematic review and meta-analysis. Parkinsonism Relat Disord 2020; 78: 12–20. doi:10.1016/j.parkreldis.2020.07.002

[16] Reiter E, Mueller C, Pinter B et al. Dorsolateral nigral hyperintensity on 3.0T susceptibility-weighted imaging in neurodegenerative Parkinsonism. Mov Disord 2015; 30: 1068–1076. doi:10.1002/mds.26171

[17] Sugiyama A, Sato N, Kimura Y et al. MR findings in the substantia nigra on phase difference enhanced imaging in neurodegenerative parkinsonism. Parkinsonism Relat Disord 2018; 48: 10–16. doi:10.1016/j.parkreldis.2017.12.021

[18] Kim JM, Jeong HJ, Bae YJ et al. Loss of substantia nigra hyperintensity on 7 Tesla MRI of Parkinson's disease, multiple system atrophy, and progressive supranuclear palsy. Parkinsonism Relat Disord 2016; 26: 47–54. doi:10.1016/j.parkreldis.2016.01.023

[19] Bae YJ, Kim JM, Kim KJ et al. Loss of Substantia Nigra Hyperintensity at 3.0-T MR Imaging in Idiopathic REM Sleep Behavior Disorder. Comparison with 123I-FP-CIT SPECT. Radiology 2018; 287: 285–293. doi:10.1148/radiol.2017162486

[20] Zucca FA, Basso E, Cupaioli FA et al. Neuromelanin of the human substantia nigra. An update. Neurotox Res 2014; 25: 13–23. doi:10.1007/s12640-013-9435-y

[21] Huddleston DE, Langley J, Dusek P et al. Imaging Parkinsonian Pathology in Substantia Nigra with MRI. Curr Radiol Rep 2018; 6: 154 doi:10.1007/s40134-018-0272-x

[22] Kim EY, Sung YH, Lee J. Nigrosome 1 imaging. Technical considerations and clinical applications. Br J Radiol 2019; 92: 20180842 doi:10.1259/bjr.20180842

[23] Xing Y, Sapuan A, Dineen RA et al. Life span pigmentation changes of the substantia nigra detected by neuromelanin-sensitive MRI. Mov Disord 2018; 33: 1792–1799. doi:10.1002/mds.27502

[24] Jin L, Wang J, Wang C et al. Combined Visualization of Nigrosome-1 and Neuromelanin in the Substantia Nigra Using 3T MRI for the Differential Diagnosis of Essential Tremor and de novo Parkinson's Disease. Front Neurol 2019; 10: 100 doi:10.3389/fneur.2019.00100

[25] Trifonova OP, Maslov DL, Balashova EE et al. Parkinson's Disease. Available Clinical and Promising Omics Tests for Diagnostics, Disease Risk Assessment, and Pharmacotherapy Personalization. Diagnostics (Basel) 2020; 10: doi:10.3390/diagnostics10050339

[26] Fabbri M, Reimão S, Carvalho M et al. Substantia Nigra Neuromelanin as an Imaging Biomarker of Disease Progression in Parkinson's Disease. J Parkinsons Dis 2017; 7: 491–501. doi:10.3233/jpd-171135

[27] Sommerauer M, Fedorova TD, Hansen AK et al. Evaluation of the noradrenergic system in Parkinson's disease. An 11C-MeNER PET and neuromelanin MRI study. Brain 2018; 141: 496–504. doi:10.1093/brain/awx348

[28] Pyatigorskaya N, Gaurav R, Arnaldi D et al. Magnetic Resonance Imaging Biomarkers to Assess Substantia Nigra Damage in Idiopathic Rapid Eye Movement Sleep Behavior Disorder. Sleep 2017; 40: doi:10.1093/sleep/zsx149

[29] Pyatigorskaya N, Gallea C, Garcia-Lorenzo D et al. A review of the use of magnetic resonance imaging in Parkinson's disease. Ther Adv Neurol Disord 2014; 7: 206–220. doi:10.1177/1756285613511507

[30] Shinde S, Prasad S, Saboo Y et al. Predictive markers for Parkinson's disease using deep neural nets on neuromelanin sensitive MRI. Neuroimage Clin 2019; 22: 101748 doi:10.1016/j.nicl.2019.101748

[31] Mochizuki H, Choong CJ, Baba K. Parkinson's disease and iron. J Neural Transm (Vienna) 2020; 127: 181–187. doi:10.1007/s00702-020-02149-3

[32] Langkammer C, Schweser F, Krebs N et al. Quantitative susceptibility mapping (QSM) as a means to measure brain iron? A post mortem validation study. Neuroimage 2012; 62: 1593–1599. doi:10.1016/j.neuroimage.2012.05.049

[33] Martin-Bastida A, Lao-Kaim NP, Loane C et al. Motor associations of iron accumulation in deep grey matter nuclei in Parkinson's disease. A cross-sectional study of iron-related magnetic resonance imaging susceptibility. Eur J Neurol 2017; 24: 357–365. doi:10.1111/ene.13208

[34] Zhao X, An H, Liu T et al. Quantitative Susceptibility Mapping of the Substantia Nigra in Parkinson's Disease. Appl Magn Reson 2017; 48: 533–544. doi:10.1007/s00723-017-0877-x

[35] Chen Q, Chen Y, Zhang Y et al. Iron deposition in Parkinson's disease by quantitative susceptibility mapping. BMC Neurosci 2019; 20: 23 doi:10.1186/s12868-019-0505-9

[36] Du G, Lewis MM, Sica C et al. Distinct progression pattern of susceptibility MRI in the substantia nigra of Parkinson's patients. Mov Disord 2018; 33: 1423–1431. doi:10.1002/mds.27318

[37] Ulla M, Bonny JM, Ouchchane L et al. Is R2* a new MRI biomarker for the progression of Parkinson's disease? A longitudinal follow-up. PLoS ONE 2013; 8: e57904 doi:10.1371/journal.pone.0057904

[38] Lee JH, Lee MS. Brain Iron Accumulation in Atypical Parkinsonian Syndromes. In vivo MRI Evidences for Distinctive Patterns. Front Neurol 2019; 10: 74 doi:10.3389/fneur.2019.00074

[39] Cochrane CJ, Ebmeier KP. Diffusion tensor imaging in parkinsonian syndromes. A systematic review and meta-analysis. Neurology 2013; 80: 857–864. doi:10.1212/wnl.0b013e318284070c

[40] Atkinson-Clement C, Pinto S, Eusebio A et al. Diffusion tensor imaging in Parkinson's disease. Review and meta-analysis. Neuroimage Clin 2017; 16: 98–110. doi:10.1016/j.nicl.2017.07.011

[41] Andica C, Kamagata K, Hatano T et al. MR biomarkers of degenerative brain disorders derived from diffusion imaging. J Magn Reson Imaging 2019. doi:10.1002/jmri.27019

[42] Ofori E, Pasternak O, Planetta PJ et al. Increased free water in the substantia nigra of Parkinson's disease. A single-site and multi-site study. Neurobiol Aging 2015; 36: 1097–1104. doi:10.1016/j.neurobiolaging.2014.10.029

[43] Zhang G, Zhang Y, Zhang C et al. Diffusion Kurtosis Imaging of Substantia Nigra Is a Sensitive Method for Early Diagnosis and Disease Evaluation in Parkinson's Disease. Parkinsons Dis 2015; 2015: 207624 doi:10.1155/2015/207624

[44] Wang JJ, Lin WY, Lu CS et al. Parkinson disease. Diagnostic utility of diffusion kurtosis imaging. Radiology 2011; 261: 210–217. doi:10.1148/radiol.11102277

[45] Chougar L, Pyatigorskaya N, Degos B et al. The Role of Magnetic Resonance Imaging for the Diagnosis of Atypical Parkinsonism. Front Neurol 2020; 11: 665 doi:10.3389/fneur.2020.00665

[46] Saeed U, Compagnone J, Aviv RI et al. Imaging biomarkers in Parkinson's disease and Parkinsonian syndromes. Current and emerging concepts. Transl Neurodegener 2017; 6: 8 doi:10.1186/s40035-017-0076-6

[47] Quattrone A, Nicoletti G, Messina D et al. MR imaging index for differentiation of progressive supranuclear palsy from Parkinson disease and the Parkinson variant of multiple system atrophy. Radiology 2008; 246: 214–221. doi:10.1148/radiol.2453061703

[48] Barbagallo G, Sierra-Peña M, Nemmi F et al. Multimodal MRI assessment of nigro-striatal pathway in multiple system atrophy and Parkinson disease. Mov Disord 2016; 31: 325–334. doi:10.1002/mds.26471

[49] Armstrong MJ. Progressive Supranuclear Palsy. An Update. Curr Neurol Neurosci Rep 2018; 18: 12 doi:10.1007/s11910-018-0819-5

[50] Kashihara K, Shinya T, Higaki F. Reduction of neuromelanin-positive nigral volume in patients with MSA, PSP and CBD. Intern Med 2011; 50: 1683–1687. doi:10.2169/internalmedicine.50.5101

[51] Mueller C, Hussl A, Krismer F et al. The diagnostic accuracy of the hummingbird and morning glory sign in patients with neurodegenerative parkinsonism. Parkinsonism Relat Disord 2018; 54: 90–94. doi:10.1016/j.parkreldis.2018.04.005

[52] Mangesius S, Hussl A, Krismer F et al. MR planimetry in neurodegenerative parkinsonism yields high diagnostic accuracy for PSP. Parkinsonism Relat Disord 2018; 46: 47–55. doi:10.1016/j.parkreldis.2017.10.020

[53] Nigro S, Arabia G, Antonini A et al. Magnetic Resonance Parkinsonism Index. Diagnostic accuracy of a fully automated algorithm in comparison with the manual measurement in a large Italian multicentre study in patients with progressive supranuclear palsy. Eur Radiol 2017; 27: 2665–2675. doi:10.1007/s00330-016-4622-x

[54] Quattrone A, Morelli M, Williams DR et al. MR parkinsonism index predicts vertical supranuclear gaze palsy in patients with PSP-parkinsonism. Neurology 2016; 87: 1266–1273. doi:10.1212/WNL.0000000000003125